

TOPICAL REVIEW • OPEN ACCESS

## A new approach towards spintronics–spintronics with no magnets

To cite this article: Karen Michaeli *et al* 2017 *J. Phys.: Condens. Matter* **29** 103002

View the [article online](#) for updates and enhancements.

### You may also like

- [Carrier localization and magnetoresistance in DNA-functionalized carbon nanotubes](#)  
Md Wazedur Rahman, Seyedamin Firouzeh and Sandipan Pramanik
- [Methods for Calculating Frequency of Maintenance of Complex Information Security System Based on Dynamics of Its Reliability](#)  
S K Varlataya, V E Evdokimov and A Y Urzov
- [Single-molecule nano-optoelectronics: insights from physics](#)  
Peihui Li, Li Zhou, Cong Zhao et al.

## Topical Review

# A new approach towards spintronics— spintronics with no magnets

Karen Michaeli<sup>1</sup>, Vaibhav Varade<sup>2</sup>, Ron Naaman<sup>2</sup> and David H Waldeck<sup>3</sup>

<sup>1</sup> Department of Condensed Matter, Weizmann Institute of Science, Rehovot 76100, Israel

<sup>2</sup> Department of Chemical Physics, Weizmann Institute of Science, Rehovot 76100, Israel

<sup>3</sup> Department of Chemistry, University of Pittsburgh, Pittsburgh, PA 15260, United States of America

E-mail: [ron.naaman@weizmann.ac.il](mailto:ron.naaman@weizmann.ac.il)

Received 7 January 2016, revised 31 October 2016

Accepted for publication 6 December 2016

Published 31 January 2017



### Abstract

We review a recently discovered phenomenon, the chiral induced spin selectivity (CISS) effect, that can enable a new technology for the injection of spin polarized current without the need for a permanent magnetic layer. The effect occurs in chiral molecules and systems without parity symmetry, i.e. systems that do not have inversion symmetry. The theoretical foundations for the effect are presented first and then followed by several examples of spin-valves that are based on chiral systems. The CISS-based spin valves introduce the possibility to inject spin current without the use of a permanent magnet and to achieve relatively large magnetoresistance at room temperature.

Keywords: spin, chirality, spintronics

(Some figures may appear in colour only in the online journal)

## 1. Introduction

Current solid-state logic relies on the use of transistors, in which capacitors are charged and discharged. Spintronics has been suggested as an alternative technology that exploits the electron spin rather than its charge, because spin manipulation ought to require less energy than charging capacitors [1]. Since the introduction of the spin transistor concept [2] much experimental and theoretical effort has been directed toward its realization; however the technology remains inferior to that of well-established charge-based transistors. Because of existing technologies, silicon is viewed as the material of choice for spintronics; however silicon's small spin-orbit coupling (SOC) results in self-contradictory properties. On the one hand, spins have a relatively long mean free path in silicon, which is necessary for a spin transistor, but on the other hand

a relatively high voltage is required to induce significant spin precession.

Producing an efficient and practical spin transistor requires that one be able to inject spins into a semiconductor with high efficiency and selectivity, reaching 100% at room temperature. Common spin injectors are made of ferromagnetic (FM) layers that intrinsically do not inject pure spin at room temperature. This limitation may be overcome by applying multiple layer configurations; however the interfacial barriers, in particular the Schottky barrier between the spin injector and the semiconductor [3, 4], can cause spin depolarization, which reduces the efficiency of the spin injector [5]. In addition, it is important to find a way to manipulate the spin in real time, e.g. by applying a relatively low voltage.

Although progress in developing spin transistors is limited, it has been possible to develop practical spintronic devices that have penetrated into two important applications, read heads in hard disks and magnetic memory. Both applications use magnetoresistive spin valves that are based on the giant magnetoresistance effect (GMR) [6] and on the tunnel



Original content from this work may be used under the terms of the [Creative Commons Attribution 3.0 licence](https://creativecommons.org/licenses/by/3.0/). Any further distribution of this work must maintain attribution to the author(s) and the title of the work, journal citation and DOI.

magnetoresistance (TMR effect) [7, 8]. In the spin valve, two FM layers are separated by a thin non-magnetic layer. The magnetic dipole of one FM layer is permanent, while the magnetic dipole of the other FM is a ‘free-layer’ and can be changed, either by an external magnetic field (in the case of the reading head) or by a spin current flowing through it, as in the case of spin torque magnetic memory [9]. The resistance of a spin valve is changed according to the magnetization direction of the free layer.

Despite the success of these memory devices and their commercial application, they suffer from intrinsic drawbacks that limit their future development. The first drawback is their limited promise for miniaturization. Because FM materials tend to become super-paramagnetic at small (nanometer) sizes, such devices are likely to be limited to areas of about 70 nm<sup>2</sup>. There is much effort to solve the problem by converting the devices from being magnetized in plane to being magnetized perpendicular to the film’s surface, however shrinking the size of the read head in hard disks remains a significant challenge. A second challenge for GMR and TMR [8] devices is the need to have a permanent magnetic film in close proximity to the free FM layer at room temperature. Current technology meets this challenge by using multiple layers of films that stabilize the permanent magnetic film by antiferromagnetic interactions. Such structures are relatively expensive to produce and they limit the expansion of these memory technologies to devices that are both higher in density and lower in cost.

In addition to the inorganic structures discussed above, considerable research has been performed in ‘organic spintronics’ in which organic molecules (or materials) serve as the dielectric layer in GMR like devices [10]. Magnetoresistance effects have also been observed in various organic based devices in some cases when the organic molecules themselves contained paramagnetic atoms [11] or even when the molecules are diamagnetic [12, 13].

This article describes a recently discovered phenomenon, the chiral induced spin selectivity (CISS) effect [14], which can enable a new technology for the injection of spin polarized current without the need for a permanent magnetic layer. The CISS effect [14] occurs in molecules without parity symmetry, i.e. systems that do not have inversion symmetry [15]. The special spectroscopic properties of chiral molecules have been appreciated since the beginning of the nineteenth century, however the influence of chiral symmetry on a molecule’s electron transport properties has only been probed for the past two decades.

Studies of electron transport through chiral molecules have been performed over a short distance range, from a few nanometers in the case of oligopeptides and proteins to about 30 nm in the case of double strand DNA, and up to a hundred nanometers in the case of carbon nanotubes wrapped with DNA [16]. The short range transport is presumed to occur by tunneling, whereas the longer range transport combines tunneling and hopping [17]. For the length range studied, the spin polarization lifetime exceeds the transport time by several orders of magnitude. In these studies, it was found that electron transport through chiral molecules is spin selective and the consequent spin polarization is very large compared to

inorganic spin filters. Note that the ratio between the transmission probability of the favored spin direction, versus the other spin direction is known to reach values of more than four to one at room temperature for DNA; a spin polarization which exceeds that of common solid-state based spin filters [18]. This phenomenon was not anticipated, as organic molecules are known for their small SOC and the molecules used are not magnetic. Hence, the experimental observations provide a challenge to theory. In what follows the effect will be described and the theory behind it will be reviewed. Subsequently, we will describe some recent results on the development of spin injectors that are based on the CISS effect.

## 2. Theory

Organic chiral molecules can serve as non-magnetic spin filters because the electron transmission probability through them strongly depends on the electron’s helicity. Electrons of a certain spin can traverse the molecule more easily in one direction than in the other (depending on the handedness of the molecule). These directions are reversed for electrons of opposite spin. This property implies strong spin-orbit interactions, and early theoretical attempts to explain the CISS effect invoked SOC with a magnitude much larger than that which one typically encounters in organic materials [19–23]. Recently a modified theory [24] has explained the high degree of spin selectivity as originating from the interplay between a helicity-induced SOC and a strong dipole electric field, which is characteristic of these molecules, or an external electric field acting on the chiral molecules. This mechanism can account for the large spin polarization measured in experiments over an energy range of hundreds of meV without relying on an unusually large SOC.

Because a chiral molecule has a helical electrostatic potential, from a symmetry perspective, their electronic properties may be understood by studying an electron gas confined to a helix-shaped narrow tube. As a consequence of this confinement, the corresponding quasi-1D Hamiltonian describes electrons moving in curved space. Crucially, this curvature entangles degrees of freedom along the tube with the ones across it, unlike a straight cylinder where they are separable. In particular, the SOC that arises from the confining potential has the familiar form  $\vec{L} \cdot \vec{S}$  where the direction of  $\vec{L}$  is tangent to the helix, and hence changes as a function of position along the helix (see figure 1). Consequently, the SOC term connects the spin  $\sigma$  to both the position  $s$  along the helix and the angular momentum  $\ell$ . The latter refers to the angular momentum perpendicular to the helix, i.e. the eigenvalue of  $L = -i\frac{\partial}{\partial\theta}$  (where  $\theta$  is the angle in the  $n$ - $t$  plane). Explicitly, the SOC term in the Hamiltonian is

$$H_{\text{SOC}} = \kappa\vec{L} \cdot \vec{S} = \kappa\ell \left[ \sigma_x \sin(2\pi s/\tilde{R}) - \sigma_y \cos(2\pi s/\tilde{R}) - \sigma_z b/2\pi\tilde{R} \right] \quad (1)$$

This term resembles a Zeeman magnetic field that rotates as a function of position. The direction of rotation is determined by the chirality of the molecule and is captured by the sign of the parameter  $\tilde{R} = \pm \sqrt{(2\pi R)^2 + b^2}$  which is positive (negative) for a right (left) handed helix;  $R$  and  $b$  are the helix’

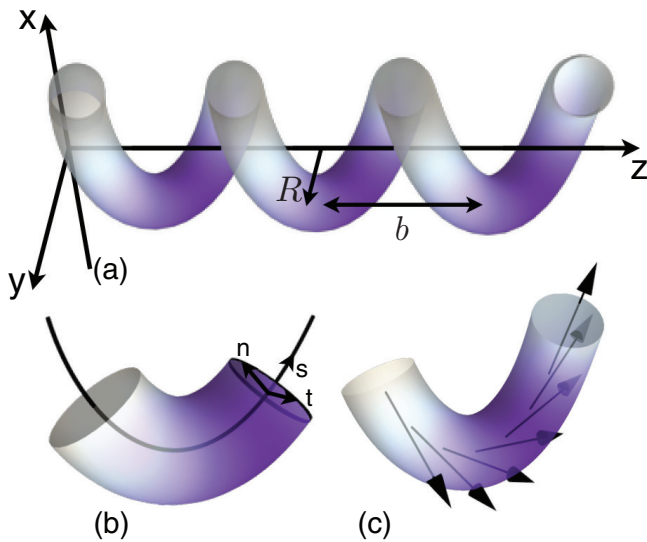


**Figure 1.** Panel (a) shows a helix-shaped tube of radius  $R$  and pitch  $b$ , corresponding to the theoretical model. Panel (b) illustrates the helical coordinate system  $(s, n, t)$ , where  $s$  is the displacement along the tube, and  $(n, t)$  spans the perpendicular plane. Panel (c) shows the effective Zeeman field created by the spin-orbit coupling (equation (1)), which is rotating as a function of position along the helix.

radius and pitch, respectively. This effective Zeeman field is the leading term that connects the electron spin and the non-relativistic dynamics, and it is closely related to the Berry curvature [25]. The coefficient  $\kappa$  is proportional to the atomic SOC which is of the order of several meV (comparable to the SOC of carbon). Interestingly, a chiral magnetic field similar to equation (1) has been shown to arise from solitons in 1D spin-chains where it results in a spin-dependent neutron scattering [26]. Performing a spin dependent gauge transformation on the wavefunction  $\Psi_\sigma(s) \rightarrow \Psi_\sigma e^{-i\pi\sigma s/\tilde{R}}$ , the SOC term splits into two contributions: a Rashba-like SOC term that is proportional to  $-i\left(\frac{2\pi}{\tilde{R}}\right)\sigma_z\partial_s$  and a constant Zeeman field  $\kappa\ell\sigma_y$ . The sign of the former is determined by the handedness of the molecule, while the sign of the latter depends on the angular momentum of the electronic state.

The energy spectrum for electrons propagating along the helix and subject to the SOC introduced above gives rise to a spin selective transmission. All energies within the  $\ell = 0$  band are four-fold degenerate, two spin states each with two opposite velocities. Thus, electrons of any spin can be transmitted through the molecule in both directions for  $\ell = 0$ . For  $\ell \neq 0$  a partial gap opens in the energy bands because of the Zeeman-like term  $\kappa\ell\sigma_y$ . Within this range of energies, the states are quasi-helical, as the spin is almost perfectly locked to the momentum direction. Because the helicity of these states is determined by the sign of the Rashba-like term (or equivalently the sign of  $\tilde{R}$ ) and independent of  $\ell$ , transmission in this energy window is strongly spin selective. The energy of the partial gap is proportional to  $\kappa \sim 1$  meV, however; and spin selectivity is only expected to be observed within a narrow range of energies and at ultra-low temperatures. We note that the Zeeman-like term is proportional to the angular momentum  $\ell$ ,

and therefore, time reversal symmetry is preserved in organic helical molecules. As a result, these systems filter electrons according to their helicity, in contrast to molecular magnets that are sensitive only to the spin of the electrons tunneling through them [27]. Moreover, since organic molecules usually carry zero net spin, effects arising from exchange coupling with the leads, such as Kondo [28] or RKKY [11] effects are not expected to occur.

The CISS effect becomes significant in organic molecules that have a dipole moment or when an external electric field is applied on the molecule. This electric field localizes the electronic states near one edge of the dipole potential, and hence reduces the conduction. However in the presence of a helicity-induced SOC (equation (1)), the helical nature of the electronic states and the partial gap in the spectrum lead to suppression in back scattering that extends up to high energies of the order of the potential barrier height. As a result, electronic states with  $\ell \neq 0$  acquire some peculiar features: (i) the amplitudes of the wavefunctions at the end of the molecule are significantly larger for  $\ell \neq 0$  than for  $\ell = 0$ , and (ii) the tails of the wavefunctions, which penetrate more deeply into the potential barrier, have a particular helicity. These features give rise to a strong spin-dependent tunneling current over an energy range that is determined by the magnitude of the electric potential drop along the molecule ( $\sim 100$  meV) rather than by  $\kappa$ .

Thus even a weak helicity-induced SOC, significantly affects electronic transport in the tunneling regime. More specifically, it both enhances the transmission probability over that of the achiral analogue, and it filters the spin of the transferred electrons.

We conclude the discussion of this theoretical model by noting a number of additional features. First, this model indicates that the CISS effect is significant only when the mechanism of electron transfer through the molecule is tunneling (this may also include hopping which consists of several consecutive tunneling events). Within this model, the CISS effect operates at high temperatures ( $kT > \text{SOC}$ ) only if the electronic states are localized, and it will become less pronounced, or even negligible, for molecules with high transmission probability. Second, the directionality generated by the locking of the electron spin and velocity suggests that backscattering by phonons or disorder is suppressed. While some experimental evidence already exists to support this feature, it has not been tested rigorously so far. Third, the spin polarization is maximal in this model when  $\pi\kappa\ell\tilde{R} \sim 1$  and it vanishes for too large SOC, destroying the CISS effect.

### 3. CISS-based spin valves

The CISS effect allows for an alternative approach to the common spin injection strategy that is used with GMR based devices. In this new approach, the permanent magnetic layer is replaced by an organic/inorganic chiral material that is non-magnetic and acts as a spin filter to provide a spin-polarized electron tunneling current [29]. There are several manifestations of this strategy. In one, a self-assembled monolayer (SAM) of chiral molecules is deposited on a non-magnetic

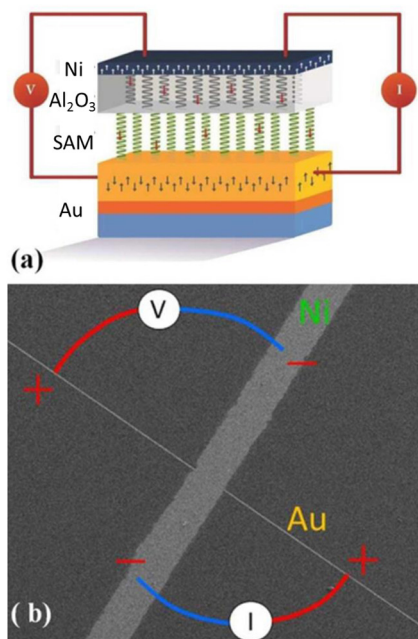


**Figure 2.** Panel (a) shows a schematic diagram of the magnetoresistance device that was used to probe the Au/SAM/Al<sub>2</sub>O<sub>3</sub> spin-injector device and the principle of the electrical resistance measurement ( $R = V/I$ ). The blue layer is Si; the yellow orange layer is Au; the more reddish orange layer is silicon oxide; the transparent and white layer are the SAM/Al<sub>2</sub>O<sub>3</sub>; and the top black layer is the Ni film. Panel (b) shows an SEM image (top view) of the device with a thin (1  $\mu$ m wide) gold trace and a wide (50  $\mu$ m) nickel trace perpendicular to it. Adapted from [29] with permission.

metal substrate and an ultrathin (1.5–2 nm) Al<sub>2</sub>O<sub>3</sub> film is grown on top of it [29]; after which, a thin FM film is deposited on top of the alumina (see figure 2). Alternatively, an ultrathin layer of conductive polymer can be spin coated on the chiral SAM and then a FM layer can be coated on top of the polymer. In a third manifestation, chiral semiconductor quantum dots (QDs) have been shown to act as spin filters when sandwiched between two metal electrodes [30]. While each of these approaches has demonstrated spin-filtering, they have their relative advantages. For example, the Al<sub>2</sub>O<sub>3</sub> films offer promise for use in electronic devices because alumina is a chemically robust oxide, however the deposition procedure must be performed at low temperatures (circa 100 °C), in order to avoid damage to the chiral SAM template, and this results in a defective film that can have pinhole electrical shorts giving rise to a device yield of about 20%. In contrast the use of a conductive polymer film as the tunnel junction increases the production yield of the devices to nearly 100%.

Figure 2 shows a schematic diagram of the spin-injector design in panel (a) and a scanning electron microscopy image of one of the Al<sub>2</sub>O<sub>3</sub> devices in panel (b). The device consists of a thin gold film electrode that is coated with a SAM of cysteine molecules. When an Al<sub>2</sub>O<sub>3</sub> layer is grown on this SAM by atomic layer deposition, it is believed that the alumina adopts a chiral structure [31, 32], however this is inferred from aspects of the film’s enantiospecific function rather than direct structural characterization. Mathew *et al* [29] evaluated the chirality of the cysteine SAM/Al<sub>2</sub>O<sub>3</sub> tunneling

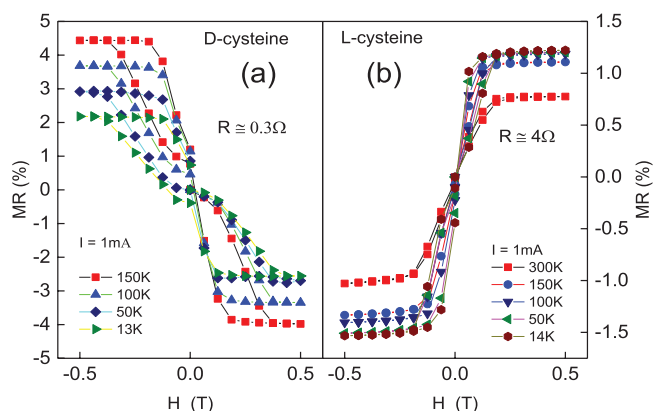


**Figure 3.** The magnetoresistance measured with a magnetic field up to 0.5 T at various fixed temperatures on devices with 2 nm-thick chiral Al<sub>2</sub>O<sub>3</sub> deposited on top of the SAM. Panel (a) shows a D-cysteine SAM on a gold surface, and panel (b) shows an L-cysteine SAM on a gold surface. Measurements were performed at constant current 1 mA. Copied from [29] with permission.

barrier by cyclic voltammetry measurements in which the Au/(L- or D-) cysteine/Al<sub>2</sub>O<sub>3</sub> was used as a working electrode in an electrochemical cell. They showed that the faradaic current which was observed for a chiral N,N-dimethyl-1-ferrocenylethylamine (R-Fc or S-Fc) redox couple displayed a sensitivity to the chirality of the Au/SAM/Al<sub>2</sub>O<sub>3</sub> working electrode. Namely, that the Au/D-cysteine/Al<sub>2</sub>O<sub>3</sub> working electrode had a higher faradaic peak current for the S-Fc than for the R-Fc; whereas the Au/L-cysteine/Al<sub>2</sub>O<sub>3</sub> L-cysteine had a higher faradaic peak current for the R-Fc than for the S-Fc.

To analyze the performance of the Au/SAM/Al<sub>2</sub>O<sub>3</sub> spin injector, Mathew *et al* [29] deposited a 150 nm thick Ni layer on top of the Al<sub>2</sub>O<sub>3</sub> and measured its resistance as a function of an applied magnetic field. The conduction through the device occurs by tunneling and the voltage drop was used to calculate the resistance. The magnetic field was applied parallel to the direction of current flow (perpendicular to the Ni film/Al<sub>2</sub>O<sub>3</sub> tunnel barrier plane), and it was used to split the nickel film’s spin sublevels. Unlike traditional FM spin injectors, the chiral tunnel barrier does not respond to the applied magnetic field, and the origin of the signal arises solely from the change in population of the Ni films spin sublevels; i.e. the Ni analyzes for the intrinsic spin polarization of the Au/SAM/Al<sub>2</sub>O<sub>3</sub> spin-injector. Figure 3 presents some of the magnetoresistance (MR) data they reported; namely  $MR \equiv [R(H) - R(H = 0)] / R(H = 0) \times 100\%$  is plotted as a function of magnetic field H for two different spin-injector chiralities at temperatures between 14 K and 300 K. Note that  $R(H)$  is defined as the resistance under a field strength H and  $R(H = 0)$  is the zero-field resistance.

Figure 3 shows the magnetoresistance data that Mathew *et al* [29] obtained for two different chirality SAM/Al<sub>2</sub>O<sub>3</sub> films, i.e. L-cysteine Al<sub>2</sub>O<sub>3</sub> and D-cysteine Al<sub>2</sub>O<sub>3</sub>. The most obvious difference between the two devices is that they have opposite signs for the MR response; i.e. the sign of the slope for the MR versus H plots are opposite to one another. This difference in the response correlates with the difference in the chirality of the cysteine molecules, which were used to template the

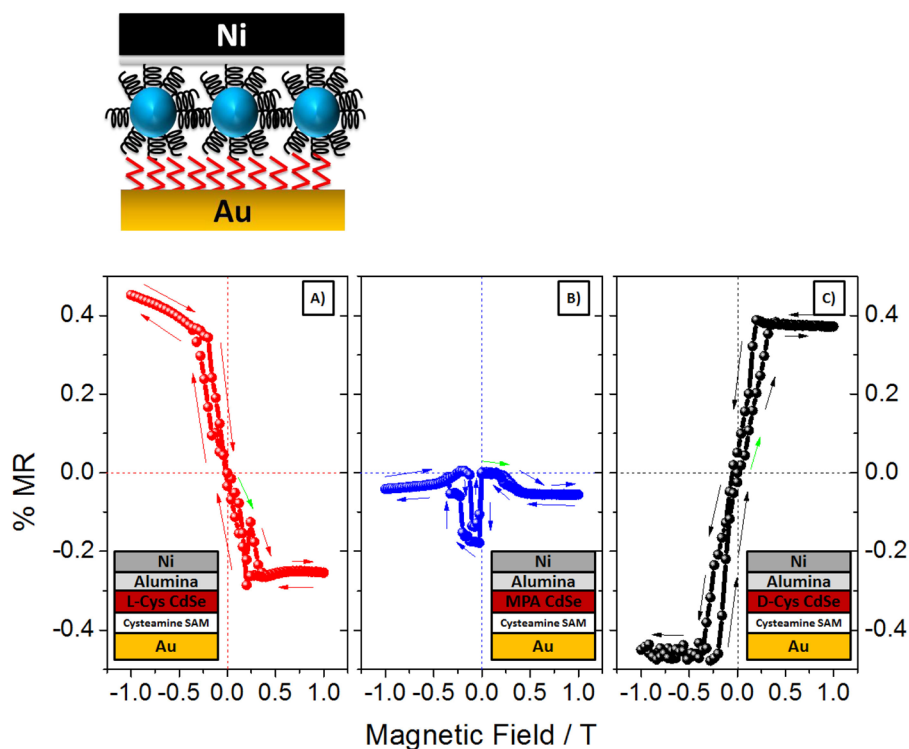


**Figure 4.** Magnetoresistance of chiral QD thin films. (Left) Schematic illustration of the cross-section of the magnetoresistance (MR) device structure. (Bottom) MR data are shown for thin films composed of L-Cysteine (A), MPA (B), and D-Cysteine (C) capped CdSe QDs at 20 K, recorded as a function of external magnetic field up to 1 T at a fixed current of 0.1 mA. The arrows indicate the scan direction, and the green arrow indicates the origin of the scan. Taken from [30], with permission.

SAM/ $\text{Al}_2\text{O}_3$  films. Moreover, the MR versus  $H$  curves are not symmetric about  $H = 0$  but are approximately antisymmetric. In typical GMR devices, the magnetoresistance does not depend on the sign of the applied magnetic field, but only on its magnitude. For the device structure illustrated in figure 2, the magnetoresistance depends on the magnetic field direction and the chirality of the tunneling barrier because the tunnel barrier, which defines the spin alignment, is not affected by the external magnetic field. For the D-cysteine/ $\text{Al}_2\text{O}_3$  barrier, the MR is high for a positive magnetic field and the MR is low for a negative magnetic field, whereas the L-cysteine  $\text{Al}_2\text{O}_3$  barrier has a low MR for a positive magnetic field and a high MR for a negative magnetic field. This difference arises because the device sketched in figure 2(A) has only the analyzing magnet (the nickel layer) and no second magnetic layer, as in a GMR device.

Qualitatively, the device works in the following manner. As the electrons transit the tunneling barrier the spin distribution becomes polarized by the CISS effect either parallel or antiparallel to their velocity, depending on the chirality of the tunneling barrier. Whether or not an electron transits into the Ni film depends on the electron's spin and the density of empty states in the nickel layer for that spin to populate; and this density of available states is controlled by the applied magnetic field and the voltage drop. Thus, the Au/SAM/ $\text{Al}_2\text{O}_3$  layers form a tunnel junction that transmits a spin polarized current and the nickel layer acts as an analyzer for that spin polarization. As the external magnetic field increases the Ni becomes more strongly magnetized (more domains are

aligned) in the field direction, and hence it has more empty spin down states near the Fermi level and is less resistive for electrons whose spin is antiparallel to the electron velocity. Thus, the D-cysteine SAM/ $\text{Al}_2\text{O}_3$  has a low resistance for positive H-field and this indicates that it selects for electron spins that are anti-parallel to the electron velocity.

This interpretation of the response is consistent with the lack of any significant temperature dependence of the MR response of the device. The data in figure 3 show that the MR changes very little with temperature over the range of 14 K–150 K. Note that the magnitude of the MR response and the interface resistance measured in the two devices are different. Mathew *et al* [29] indicate that reproducibility in the device manufacture remains a challenge, but that the devices, once manufactured, are robust—operating for more than three months. Challenges to device fabrication arise from making a compact  $\text{Al}_2\text{O}_3$  film which is free of pinholes, maintaining a low surface roughness of the  $\text{Al}_2\text{O}_3$  film and controlling the microstructure of the Ni film. Indeed, especially efficient spin valves were also produced but with low yield because of the irreproducible  $\text{Al}_2\text{O}_3$  layer.

A second type of CISS based spin valve is shown in figure 4. In this case chiral QDs [33, 34] serve as the spin filtering element, which is sandwiched between a Au bottom electrode and a Ni top electrode that serves as the spin analyzer element. While semiconducting QDs have been used in spin selective charge transport devices in other works [35–37], those studies consisted of achiral QD assemblies on chiral molecular films acting as a spin filter. For the work shown in figure 4 a

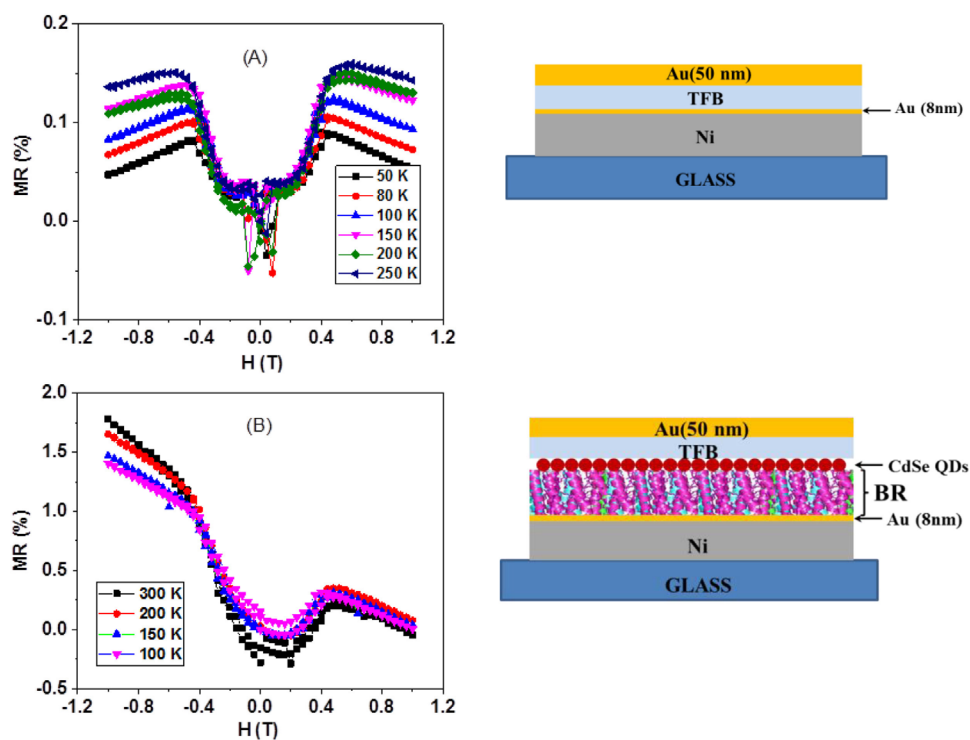


**Figure 5.** (A) Magnetoresistance (MR) curves are shown for a device that contains only conductive polymer. (B) The magnetoresistance curves are shown for a device containing the purple membrane with the bacteriorhodopsin (BR). On the right side of each panel, schemes of the devices are shown. Please note the different scale of MR in the two graphs.

ligand capping layer was used to control the electronic chirality of the QD; namely an L-cysteine ligand shell gave the L QD (figure 4(A)), a D-cysteine ligand shell gave the D QD (figure 4(C)), and the achiral ligand mercaptopropionic acid gave the achiral QD (figure 4(B)). Figure 4 shows MR measurements recorded as a function of applied external magnetic field for the three different cases. Note that mercaptopropionic acid differs from cysteine by the replacement of the amine group on the cysteine with a hydrogen, which makes it achiral; however its surface binding thiolate group and its length is similar to cysteine. The resistance was measured at a constant current (of  $100 \mu\text{A}$ ) through the sample, and the external magnetic field was varied from  $-1 \text{ T}$  to  $1 \text{ T}$ .

The MR curves, as a function of the external magnetic field, show that the devices with chiral ligands and the device with the achiral MPA are qualitatively different. The L-cysteine and D-cysteine CdSe QDs show opposite behaviors for the magnetoresistance, and it can be understood from their spin filtering properties, similar to the results shown in figure 2. Note that the MR plots are not entirely anti-symmetric about zero magnetic field; e.g. the L-cysteine QDs have a positive MR that saturates at approximately  $0.4\%$  and a negative MR that saturates at approximately  $-0.3\%$ . This behavior may arise because of the asymmetric tunnel barrier for the device, namely Au as the bottom contact and Ni as the top contact influencing the spin injection properties. While the chiral QD devices show an approximately anti-symmetric MR response, the achiral QDs show a symmetric MR response. The symmetric response for CdSe/CdS core-shell nanoparticles has been reported previously [38, 39], and the shape of the response has been attributed to a spin blockade mechanism which depends

on field magnitude but is not dependent on the field orientation. Note that the QD films were about  $50\%$  coverage, or less, in this study and the magnitude of the MR response might be improved if more dense films or multilayer films were studied.

Interestingly, if one considers the chirality of the cysteine molecules alone then the magnetoresistance results shown in figure 4 for the cysteine capped QDs are opposite in direction to those for the  $\text{Al}_2\text{O}_3$  coated SAMs shown in figure 3. This difference correlates with the inversion in the Cotton effect observed for cysteine bound to the CdSe QD surface as compared to free cysteine. Namely, the sign of the circular dichroism signal is opposite for the molecules in solution and for the case when the molecules are attached to the QD. This observation suggests that the asymmetry in the MR signal is associated with the chirality of the electronic state and that the charge transport through the QDs occurs through a chiral pathway.

Figure 5 shows data for a third type of MR device that is comprised of an organic spin filter layer. Formation of reproducible ‘sandwich’ like devices with organic molecules has been a challenge, because the deposition of metals or metal oxides can damage the organic molecules and their organization on a surface [40–44]. In recent studies, we found that a good alternative to atomic layer deposition or evaporation of oxides or metals is the use of a conductive polymer that is spin coated on top of the organic layer and then protects it from the metal film that is deposited on the conductive polymer. Figure 5 presents the MR signal obtained with a device in which a film made from purple membrane that includes bacteriorhodopsin is deposited on top of a FM substrate and the top contact is made from conductive polymer. A gold electrode is

deposited on top of the polymer. Panel (A) shows the symmetric response that is expected for the achiral conductive polymer film; i.e. it does not spin filter the electron current. In contrast, the MR curves in panel (B) are asymmetric; i.e. it shows an interesting dependence that results from a superposition of the MR obtained with chiral molecules in the bacteriorhodopsin film (see e.g. figure 3) and the reference response obtained with achiral organic molecules, the polymer in this case (see figure 5(A)) [13, 45, 46]. The results clearly indicate that in the case of the device with the chiral bacteriorhodopsin (BR), the electrons transmitted from the substrate through the chiral molecules are spin polarized.

#### 4. Summary

The creation, manipulation, and detection of spin current in nanostructures are the major aspects of spintronics. We presented here a new scheme for improving the performance of spin injectors and simplifying their production. These chiral-based spin injectors should allow for an increase in the density of memory devices [47–51]. The devices presented here operate on spins polarized parallel or antiparallel to their velocity and therefore can serve as an important building block for magnetic memory which is based on perpendicular magnetization, namely elements that are magnetized perpendicular to their surfaces. They also introduce the possibility of injecting spins from insulators or semiconductors, as well as metals, making the interfacing of the spin injector with semiconductor devices much easier. Because CISS based spin valves include only a single FM layer, their use as reading heads for hard disks allow for miniaturization to a single molecule dimension, in principle.

#### Acknowledgments

This work was funded, in part, by the US Department of Energy (Grant No. ER46430). RN acknowledges the partial support from the European Research Council under the European Union's Seventh Framework Program (FP7/2007-2013)/ERC grant agreement no (338720) and the from the VW Foundation (VW 88 367).

#### References

- [1] Bandyopadhyay S and Cahay M 2009 Electron spin for classical information processing: a brief survey of spin-based logic devices, gates and circuits *Nanotechnology* **20** 412001
- [2] Datta S and Das B 1990 Electronic analog of the electro-optic modulator *Appl. Phys. Lett.* **56** 665–7
- [3] Dery H and Sham L J 2007 Spin extraction theory and its relevance to spintronics *Phys. Rev. Lett.* **98** 046602
- [4] Tran M, Jaffrès H, Deranlot C, George J M, Fert A, Miard A and Lemaître A 2009 Enhancement of the spin accumulation at the interface between a spin-polarized tunnel junction and a semiconductor *Phys. Rev. Lett.* **102** 036601
- [5] Dankert A, Dulal R S and Dash S P 2013 Efficient spin injection into silicon and the role of the Schottky barrier *Sci. Rep.* **3** 1–8
- [6] Fert A 2008 Origin, development, and future of spintronics (Nobel lecture) *Rev. Mod. Phys.* **80** 1517
- [7] Moodera J S, Kinder L R, Wong T M and Meservey R 1995 Large magnetoresistance at room temperature in ferromagnetic thin film tunnel junctions *Phys. Rev. Lett.* **74** 3273–6
- [8] Miyazaki T and Tezuka N 1995 Giant magnetic tunneling effect in Fe/Al<sub>2</sub>O<sub>3</sub>/Fe junction *J. Magn. Magn. Mater.* **139** L231
- [9] Kent A D and Worledge D C 2015 A new spin on magnetic memories *Nat. Nanotechnol.* **10** 187–9
- [10] Sun D, Ehrenfreund E and Vardeny Z V 2014 The first decade of organic spintronics research *Chem. Commun.* **50** 1781–93
- [11] Tyagi P, Baker C and D'Angelo C 2015 Paramagnetic molecule induced strong antiferromagnetic exchange coupling on a magnetic tunnel junction based molecular spintronics device *Nanotechnology* **26** 305602
- [12] Santos T S, Lee J S, Migdal P, Lekshmi I C, Satpati B and Moodera J S 2007 Room-temperature tunnel magnetoresistance and spin-polarized tunneling through an organic semiconductor barrier *Phys. Rev. Lett.* **98** 016601
- [13] Wagemans W *et al* 2011 The many faces of organic magnetoresistance *SPIN* **01** 93
- [14] Naaman R and Waldeck D H 2015 Spintronics and chirality: spin selectivity in electron transport through chiral molecules *Annu. Rev. Phys. Chem.* **66** 263–81
- [15] Bentley R 1995 From optical activity in quartz to chiral drugs: molecular handedness in biology and medicine *Perspect. Biol. Med.* **38** 188
- [16] Alam K M and Pramanik S 2015 Spin filtering through single-wall carbon nanotubes functionalized with single-stranded DNA *Adv. Funct. Mater.* **25** 3210–8
- [17] Wierzbinski E, Venkatramani R, Davis K L, Bezer S, Kong J, Xing Y, Borguet E, Achim C, Beratan D N and Waldeck D H 2013 The single-molecule conductance and electrochemical electron-transfer rate are related by a power law *ACS Nano* **7** 5391–401
- [18] Naaman R and Waldeck D H 2012 Chiral-induced spin selectivity effect *J. Phys. Chem. Lett.* **3** 2178–87
- [19] Medina E, López F, Ratner M A and Mujica V 2012 Chiral molecular films as electron polarizers and polarization modulators *Europhys. Lett.* **99** 17006
- [20] Gutierrez R, Díaz E, Naaman R and Cuniberti G 2012 Spin-selective transport through helical molecular systems *Phys. Rev. B* **85** 081404
- [21] Eremko A A and Loktev V M 2013 Spin sensitive electron transmission through helical potentials *Phys. Rev. B* **88** 1–5
- [22] Rai D and Galperin M 2013 Electrically driven spin currents in DNA *J. Phys. Chem. C* **117** 13730–7
- [23] Medina E, Gonzalez-Arraga L A, Finkelstein-Shapiro D, Berche B and Mujica V 2015 Continuum model for chiral induced spin selectivity in helical molecules *J. Chem. Phys.* **142** 194308
- [24] Michaeli K and Naaman R 2015 Origin of spin dependent tunneling through chiral molecules arXiv:1512.03435
- [25] Bradlyn B and Read N 2015 Topological central charge from Berry curvature: gravitational anomalies in trial wave functions for topological phases *Phys. Rev. B* **91** 165306
- [26] Braun H-B, Kulda J, Roessli B, Visser D, Krämer K W, Güdel H-U and Böni P 2005 Emergence of soliton chirality in a quantum antiferromagnet *Nat. Phys.* **1** 159
- Braun H-B 2012 Topological effects in nanomagnetism: from superparamagnetism to chiral quantum solitons, *Adv. Phys.* **61** 1

- [27] Heersche H B, de Groot Z, Folk J A, van der Zant H S J, Romeike C, Wegewijs M R, Zobbi L, Barreca D, Tondello E and Cornia A 2006 Electron transport through single Mn<sub>12</sub> molecular magnets *Phys. Rev. Lett.* **96** 206801
- [28] Pasupathy A N, Bialczak R C, Martinek J, Grose J E, Donev L A K, McEuen P L and Ralph D C 2004 The Kondo effect in the presence of ferromagnetism *Science* **306** 86–9
- [29] Mathew S P, Mondal P C, Moshe H, Mastai Y and Naaman R 2014 Non-magnetic organic/inorganic spin injector at room temperature *Appl. Phys. Lett.* **105** 242408
- [30] Bloom B P, Kiran V, Varade V, Naaman R and Waldeck D H 2016 Spin selective charge transport through cysteine capped CdSe quantum dots *Nano Lett.* **16** 4583
- [31] Moshe H, Vanbel M, Valev V K, Verbiest T, Dressler D and Mastai Y 2013 Chiral thin films of metal oxide *Chemistry* **19** 10295–301
- [32] Moshe H, Levi G, Sharon D and Mastai Y 2014 Atomic layer deposition of enantioselective thin film of alumina on chiral self-assembled-monolayer *Surf. Sci.* **629** 88–93
- [33] Moloney M P, Gun'ko Y K and Kelly J M 2007 Chiral highly luminescent CdS quantum dots *Chem. Commun.* **7345** 3900–2
- [34] Milton F P, Govan J, Mukhina M V, Gun'ko Y K 2016 The chiral nano-world: chiroptically active quantum nanostructures *Nanoscale Horizons* **1** 14–26
- [35] Mtangi W, Kiran V, Fontanesi C and Naaman R 2015 Role of the electron spin polarization in water splitting *J. Phys. Chem. Lett.* **4916**–22
- [36] Ben Dor O, Morali N, Yochelis S, Baczewski L T and Paltiel Y 2014 Local light-induced magnetization using nanodots and chiral molecules *Nano Lett.* **14** 6042–9
- [37] Peer N, Dujovne I, Yochelis S and Paltiel Y 2015 Nanoscale charge separation using chiral molecules *ACS Photonics* **2** 1476–81
- [38] Pourret A, Ramirez A and Guyot-Sionnest P 2009 Magnetoresistance of CdSe/CdS quantum dot films *Appl. Phys. Lett.* **95** 142105
- [39] Liu H and Guyot-Sionnest P 2015 Magnetoresistance of manganese-doped colloidal quantum dot films *J. Phys. Chem. C* **119** 14797–804
- [40] Zhou C, Deshpande M R, Reed M A, Jones L and Tour J M 1997 Nanoscale metal/self-assembled monolayer/metal heterostructures *Appl. Phys. Lett.* **71** 611
- [41] Akkerman H B, Blom P W M, de Leeuw D M and de Boer B 2006 Towards molecular electronics with large-area molecular junctions *Nature* **441** 69–72
- [42] De Boer B, Frank M M, Chabal Y J, Weirong J, Garfunkel E and Bao Z 2004 Metallic contact formation for molecular electronics: interactions between vapor-deposited metals and self-assembled monolayers of conjugated mono- and dithiols *Langmuir* **20** 1539–42
- [43] Neuhausen A B, Hosseini A, Sulpizio J A, Chidsey C E D and Goldhaber-Gordon D 2012 Molecular junctions of self-assembled monolayers with conducting polymer contacts *ACS Nano* **6** 9920–31
- [44] Cui X D, Zarate X, Tomfohr J, Sankey O F, Primak A, Moore A L, Moore T A, Gust D, Harris G and Lindsay S M 2002 Making electrical contacts to molecular monolayers *Nanotechnology* **13** 5–14
- [45] Wohlgenannt M 2012 Organic magnetoresistance and spin diffusion in organic semiconductor thin film devices *Phys. Status Solidi RRL* **6** 229–42
- [46] Wang Y, Harmon N J, Sahin-Tiras K, Wohlgenannt M and Flatt M E 2014 Anomalous organic magnetoresistance from competing carrier-spin-dependent interactions with localized electronic and nuclear spins *Phys. Rev. B* **90** 060204
- [47] Ben Dor O, Yochelis S, Mathew S P, Naaman R, Paltiel Y 2013 A chiral-based magnetic memory device without a permanent magnet *Nat. Commun.* **4** 2256
- [48] Mangin S, Ravelosona D, Katine J A and Fullerton E E 2006 Current-induced magnetization reversal in nanopillars with perpendicular anisotropy *Nat. Mater.* **5** 210
- [49] Meng H and Wang J P 2006 Spin transfer in nanomagnetic devices with perpendicular anisotropy *Appl. Phys. Lett.* **88** 172506
- [50] Sbiaa R, Lua S Y H, Law R, Meng H, Lye R and Tan H K 2011 *J. Appl. Phys.* **109** 07C707
- [51] Thomas L *et al* 2014 Perpendicular spin transfer torque magnetic random access memories with high spin torque efficiency and thermal stability for embedded applications *J. Appl. Phys.* **115** 172615